Acta Crystallographica Section F
Structural Biology and Crystallization Communications
ISSN 1744-3091

Crystallization and preliminary crystallographic analysis of *cg*Hle, a homoserine acetyltransferase homologue, from *Corynebacterium glutamicum*

Christine Tölzer,[a]‡ Sonia Pal,[a]‡ Hildegard Watzlawick,[b] Josef Altenbuchner[b]* and Karsten Niefind[a]*

[a]Universität zu Köln, Department für Chemie, Institut für Biochemie, Zülpicher Strasse 47, D-50674 Köln, Germany, and [b]Universität Stuttgart, Institut für Industrielle Genetik, Allmandring 31, D-70569 Stuttgart, Germany

‡ These authors contributed equally.

Correspondence e-mail: josef.altenbuchner@iig.uni-stuttgart.de, karsten.niefind@uni-koeln.de

Received 20 October 2008
Accepted 21 November 2008

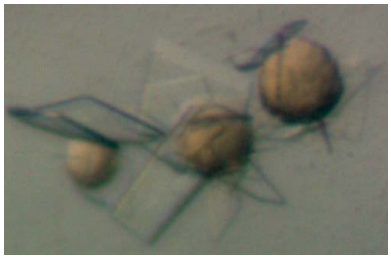

*Cg*Hle is an enzyme that is encoded by gene *cg0961* from *Corynebacterium glutamicum*. The physiological function of *cg*Hle is so far unclear. Bioinformatic annotations based on sequence homology indicated that *cg*Hle may be an acetyl-CoA:homoserine acetyl transferase and as such may be involved in methionine biosynthesis, but recent evidence has shown that it is an esterase that catalyzes the hydrolysis of acetyl esters. Here, the crystallization of *cg*Hle in two orthorhombic crystal forms, a trigonal crystal form and a monoclinic crystal form is described. The trigonal crystals have a solvent content of 83.7%, which is one of the highest solvent contents ever found for protein crystals. One of the orthorhombic crystals diffracted X-rays to at least 1.2 Å resolution.

1. Introduction

Corynebacterium glutamicum is a Gram-positive prokaryote that is of great biotechnological importance owing to its ability to produce and release glutamate and other amino acids (Hermann, 2003). The genome of *C. glutamicum* has been sequenced twice (Kalinowski *et al.*, 2003; Ikeda & Nakagawa, 2003) and many of its genes have been functionally annotated on the basis of sequence homology.

One of these genes is called *cg0961* in the KEGG database (Kanehisa *et al.*, 2008). The corresponding accession codes of the *cg0961* gene product are Q8NS43 in the UniProt knowledge base (The UniProt Consortium, 2008) and YP_225131 in the NCBI protein database, which is available *via* the NCBI's Entrez database system (http://www.ncbi.nlm.nih.gov/Entrez). Basic information about the protein encoded by *cg0961* extracted from these databases is that it comprises 349 amino acids with a calculated molecular weight of 38 836 Da and a predicted α/β-hydrolase fold (Ollis *et al.*, 1992).

Here, we describe the crystallization of this protein, which is designated as a homoserine acetyltransferase (HAT) in all three databases (KEGG, UniProt and the NCBI protein database). This annotation is based on the protein's sequence identity of nearly 30% to HAT enzymes. HAT activity is required in the methionine-biosynthesis pathway; therefore, genes that encode genuine HAT enzymes are typically called *metX* (sometimes *metA*). However, many bacteria, including *C. glutamicum*, also contain paralogues of *metX*; these paralogues are assumed to be involved in an alternative route of the methionine-biosynthesis pathway and are therefore called *met2*.

cg0961 was an obvious candidate for the *met2* gene of *C. glutamicum*. However, while the *metX* gene of *C. glutamicum* (*cg0754* in KEGG) has been unambiguously demonstrated both to play a role in methionine biosynthesis (Rückert *et al.*, 2003) and to encode a bona fide HAT enzyme (Park *et al.*, 1998), neither of these has been demonstrated for *cg0961*. On the contrary, the possibility that *cg0961* encodes an enzyme that catalyzes a step in the main or in an alternative route of the methionine pathway has been ruled out by deletion and complementation experiments (Rückert *et al.*, 2003). Thus, the annotation of the *cg0961* gene and the corresponding protein as stored in the aforementioned databases is incorrect.

We detected a probably more reliable hint concerning the function of the *cg0961*-derived protein in the Conserved Domain Database

Table 1
Crystallization of *cg*Hle and X-ray diffraction of *cg*Hle crystals.

Values in parentheses are for the highest resolution shell.

Crystal No.	1	2	3	4
Reservoir composition	24%(*w*/*v*) PEG 8000, 0.2 *M* magnesium acetate, 0.1 *M* sodium cacodylate pH 6.6	24%(*w*/*v*) PEG 8000, 0.2 *M* magnesium acetate, 0.1 *M* sodium cacodylate pH 6.6	24%(*w*/*v*) PEG 4000, 20%(*v*/*v*) glycerol, 0.16 *M* $MgCl_2$, 80 m*M* Tris–HCl pH 8.5	25.5%(*w*/*v*) PEG 4000, 15%(*v*/*v*) glycerol, 0.17 *M* lithium sulfate, 85 m*M* Tris–HCl pH 8.5
Drop composition before equilibration	0.8 µl *cg*Hle solution, 0.4 µl reservoir solution, 0.4 µl 20 m*M* acetyl-CoA, 0.48 µl 30%(*v*/*v*) ethylene glycol	0.8 µl *cg*Hle solution, 0.4 µl reservoir solution, 0.1 µl 30%(*v*/*v*) ethylene glycol	0.8 µl *cg*Hle solution, 0.4 µl reservoir solution	0.8 µl *cg*Hle solution, 0.4 µl reservoir solution
Cryoprotectant solution	24%(*w*/*v*) PEG 8000, 0.2 *M* magnesium acetate, 0.1 *M* sodium cacodylate, 20%(*v*/*v*) ethylene glycol pH 6.6	24%(*w*/*v*) PEG 8000, 0.2 *M* magnesium acetate, 0.1 *M* sodium cacodylate, 20%(*v*/*v*) ethylene glycol pH 6.6	—	—
Beamline	X12, EMBL, Hamburg	X12, EMBL, Hamburg	14.1, BESSY, Berlin	14.1, BESSY, Berlin
Wavelength (Å)	0.90000	0.90000	0.91841	0.91841
Space group	$P2_1$	$P2_12_12_1$	$P2_12_12_1$	$P3_121$ or $P3_221$
Unit-cell parameters (Å, °)	*a* = 56.79, *b* = 71.79, *c* = 91.14, β = 92.82	*a* = 72.47, *b* = 98.96, *c* = 105.41	*a* = 44.15, *b* = 89.58, *c* = 322.62	*a* = 143.57, *b* = 143.5, *c* = 197.86
V_M (Å^3 Da^{-1})	2.39	2.43	2.05	7.52
Solvent content (%)	48.6	49.5	40.1	83.7
Resolution range (Å)	20.0–2.0 (2.07–2.00)	51.2–1.2 (1.24–1.20)	45.0–1.9 (1.97–1.90)	48.5–3.3 (3.42–3.30)
R_{merge} (%)	17.0 (44.6)	11.5 (62.8)	17.7 (76.7)	12.9 (79.2)
Completeness (%)	97.2 (93.9)	98.3 (96.9)	92.6 (93.0)	100 (100)
Redundancy	3.1 (2.9)	6.9 (5.2)	9.4 (9.5)	9.4 (8.7)
Signal-to-noise ratio [$I/\sigma(I)$]	6.3 (2.2)	16.0 (2.3)	11.8 (2.3)	18.8 (2.4)
Wilson *B* factor (Å^2)	10.4	7.8	16.8	100.1

(Marchler-Bauer *et al.*, 2007), which is also part of the NCBI database system. An inquiry in this database identifies the protein as a member of the esterase/lipase superfamily. This information derives from the fact that the *cg0961*-encoded protein has a sequence identity of about 60% to the esterase MekB from *Pseudomonas veronii*, which is involved in the degradation of alkyl methyl ketones by this strain (Onaca *et al.*, 2007). In fact, like MekB, the *cg0961*-derived protein catalyzes the *in vitro* hydrolysis of *p*-nitrophenyl acetates. Hence, it cannot be excluded that the protein operates as an esterase rather than as a transferase *in vivo*.

Taken together, information retrieval from the literature and from standard life-science databases about the function of the *cg0961*/*met2* gene leads to incomplete, partly contradictory and thus confusing results. To summarize current knowledge about the gene product, we refer to it as HAT-like esterase from *C. glutamicum* (*cg*Hle) from here on. The *cg*Hle crystallization we describe here is part of a comprehensive effort to clarify the function of the enzyme using enzymological and structural methods. The latter approach will involve a detailed structural comparison of *cg*Hle with genuine HAT enzymes, two of which have been structurally characterized to date (Mirza *et al.*, 2005; Wang *et al.*, 2007).

2. Materials and methods

2.1. Expression of the *cg0961* gene

The *cg0961* gene was amplified by PCR with genomic DNA from *C. glutamicum* ATCC13032 serving as template. The gene-specific primers S4709, 5′-AAACATATGCTCGACAATAGTTTTTAC-3′, and S4711, 5′-GCAAGCTTAGCTCTCGAACAGC-3′, were used in this reaction, which introduced an additional *Nde*I restriction site at the putative N-terminal *cg0961* sequence and a *Hin*dIII restriction site just behind the putative stop codon. The 1052 bp fragment was inserted into the L-rhamnose-inducible expression vector JOE2702 (Volff *et al.*, 1996), which was cut with the appropriate restriction enzymes to create the plasmid pHWG771. *Escherichia coli* JM109 transformed with pHWG771 was used for the expression of *cg*Hle. Cells were grown at 310 K to an OD_{600} of 0.3 in 200 ml 2×YT medium containing 100 µg ml^{-1} ampicillin. *Cg*Hle production was induced by the addition of 0.1%(*w*/*v*) rhamnose and cultivation continued for 4 h at 303 K. Cells were harvested by centrifugation, washed and resuspended in 20 ml 10 m*M* potassium phosphate buffer pH 6.5 and stored at 253 K.

2.2. Purification of *cg*Hle

Recombinant *E. coli* cells were lysed by passing them twice through a French press cell at 7 MPa. Crude cell-free extract was obtained from the supernatant following centrifugation at 11 950*g* for 30 min at 277 K. The proteins in the supernatant were fractionated by anion-exchange chromatography. 40 mg crude cell-free extract was applied onto a Fractogel EMD-DMAE 150-10 column (Merck) pre-equilibrated with 10 m*M* potassium phosphate buffer pH 6.5. Bound proteins were eluted with an NaCl gradient (0–1 *M*) in the same buffer. 1 ml fractions were collected and tested for esterase activity. Active fractions were combined and further purified on a MonoQ HR 5/5 column (GE Healthcare) applying the same buffer gradient and tested further for purity by SDS–PAGE. The fractions containing the purified protein were combined, dialyzed against 10 m*M* HEPES buffer pH 7.0 and concentrated to a final protein concentration of 12.9 mg ml^{-1} by ultrafiltration on Centricon YM-10 devices (Millipore). The protein concentration was determined by the method of Bradford (1976) with bovine serum albumin as a standard.

2.3. Gel-filtration chromatography

We determined the native molecular weight of *cg*Hle by gel-filtration chromatography with a Superdex 200 10/300 GL column (GE Healthcare). The column was equilibrated with a solution containing 150 m*M* NaCl, 5%(*v*/*v*) glycerol, 10 m*M* imidazole pH 6.5, which also served for elution. A calibration run was performed with ferritin (440 kDa), catalase (240 kDa), bovine serum albumin (66 kDa) and cytochrome *c* (12.4 kDa) as molecular-weight marker proteins.

2.4. Enzyme-activity assay

The esterase activity of *cg*Hle was determined by measuring the rate of *p*-nitrophenyl acetate (pNp-Ac) hydrolysis. The assay was performed in 1 ml 0.1 *M* sodium phosphate buffer pH 6.5 at 298 K with 1 m*M* pNp-Ac. The reaction was started by adding the enzyme solution. The progress of pNp-Ac hydrolysis was followed by measuring the absorption at 410 nm in 10 s intervals for a total period of 2 min. One unit is defined as the amount of enzyme required to hydrolyse 1 µmol of pNp-Ac per minute.

2.5. Crystallization

For crystallization, the concentrated *cg*Hle stock solution was diluted with 1 m*M* tris-(2-carboxyethyl)phosphine hydrochloride (TCEP) solution to a final protein concentration of 5 mg ml^{-1}. All crystallization experiments were performed at 293 K using the sitting-drop variant of the vapour-diffusion method. For initial screening, we used various sparse-matrix and grid screens from Hampton Research.

2.6. Collection and processing of X-ray diffraction data

Crystals were prepared for diffraction experiments by flash-freezing in liquid nitrogen. Depending on whether cryoprotectants were present in sufficient concentrations in the mother liquor, the crystals were transferred to liquid nitrogen either directly from the crystallization drops (crystals 3 and 4 in Table 1) or after a quick soak in a cryoprotectant solution (crystals 1 and 2 in Table 1). X-ray diffraction data were collected either on beamline X12 of the EMBL Outstation in Hamburg (crystals 1 and 2 in Table 1) or on beamline BL14.2 of BESSY, Berlin (crystals 3 and 4 in Table 1). A MAR 224 CCD detector was mounted on both beamlines. The data-collection temperature was 100 K. The raw diffraction data were indexed and integrated with *DENZO* and scaled with *SCALEPACK* (Otwinowski *et al.*, 1997). Wilson scaling and transformation to structure-factor amplitudes were performed using *TRUNCATE* from the *CCP*4 package (Collaborative Computational Project, Number 4, 1994).

2.7. Solvent-content analysis and Patterson searches

V_M values (Matthews, 1968) were calculated for the *cg*Hle crystals in order to estimate the numbers of protomers per asymmetric unit and the solvent contents of the crystals. Furthermore, in order to detect local twofold rotation axes we computed self-rotation functions with *GLRF* (Tong & Rossmann, 1997) in polar-angle mode and restricted to a κ angle of 180°. The resolution range was 15–4 Å in all cases. For some crystal forms additional native Patterson functions were calculated and analysed with corresponding programs from the *CCP*4 suite (Collaborative Computational Project, Number 4, 1994). The high-resolution limit of these maps was 6 Å.

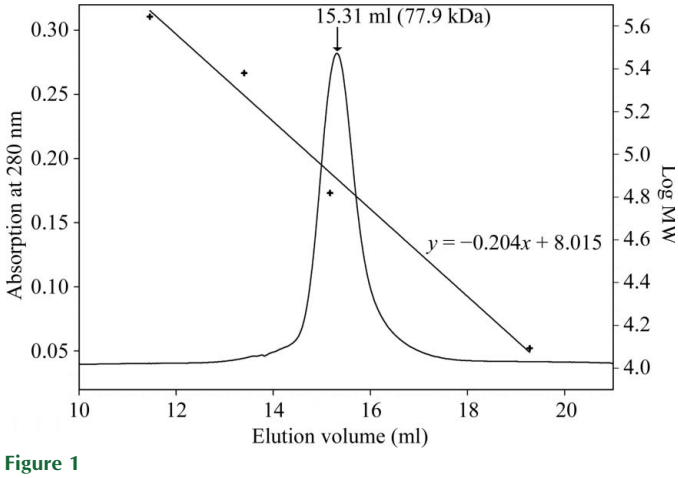

Figure 1
Molecular-weight determination of *cg*Hle by gel-filtration chromatography. The figure shows an overlay of the chromatogram with a calibration curve obtained using four proteins (ferritin, 440 kDa; catalase, 240 kDa; bovine serum albumin, 66 kDa; cytochrome *c*, 12.4 kDa). The *cg*Hle peak corresponds to a molecular weight of 77.9 kDa.

3. Results and discussion

The bacterial expression system for the *cg0961* gene was highly effective: according to an SDS–PAGE analysis (not shown), approximately 20% of the cellular protein was *cg*Hle. On the basis of this overexpression, two successive anion-chromatography steps with different column materials were sufficient to purify *cg*Hle to at least 95% homogeneity. The chromatogram of a final analytical gel-filtration run shown in Fig. 1 documents the high quality of the preparation.

The catalytic activity remained stable over a period of a few months and was also not significantly impaired by freezing. According to the gel-filtration run (Fig. 1), the native molecular weight of *cg*Hle is 77.9 kDa, which corresponds almost perfectly to a dimeric quaternary structure similar to those of the homologous homoserine acetyltransferases (Mirza *et al.*, 2005; Wang *et al.*, 2007).

Four different crystal forms of *cg*Hle could be obtained. The optimized crystallization conditions are listed in Table 1. The growth of crystal forms 1 and 2 was strictly dependent on the presence of magnesium acetate in the crystallization mixture. In many cases, we observed a kind of Ostwald ripening phenomenon (Ostwald, 1897): after 1 d of equilibration brownish spherulites appeared in the crystallization drops from which larger crystals grew after a while (Fig. 2). In many cases the spherulites finally converted completely to single crystals which could be used for diffraction experiments.

All crystals were frozen in liquid nitrogen either after transfer to cryoprotectant solutions (crystal forms 1 and 2; Table 1) or after direct harvesting from the crystallization drop (crystal forms 3 and 4). In the case of crystal forms 1 and 2 an annealing procedure comprising several rounds of thawing and refreezing (Harp *et al.*, 1999) was helpful in improving the quality of the X-ray diffraction images.

X-ray diffraction data sets were collected from all four crystal forms; their characteristics are documented in Table 1. The best resolution (1.2 Å) was achieved with crystal form 2, which promises a *cg*Hle structure of high quality. Scaling of the diffraction data from crystals 1 and 3 led to R_{merge} values of more than 17% (Table 1).

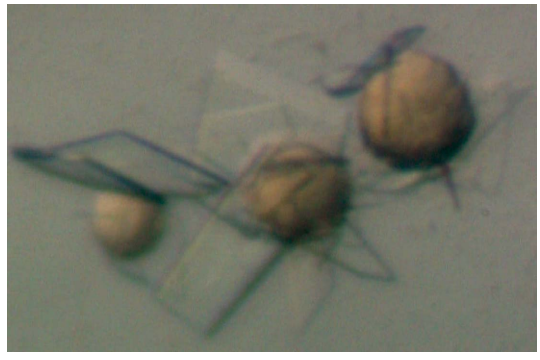

Figure 2
Crystals of *cg*Hle during growth from initially formed spherulites. The crystals belong to the orthorhombic form 2 (Table 1).

Plausible explanations of these relatively large values are the high redundancy of the data set in the case of crystal form 3 (Table 1) and impurities in the diffraction images of crystal form 1, *i.e.* strange spots that did not fit into the main diffraction pattern and originated from small twin crystals.

The dimeric nature of *cg*Hle led us to calculate self-rotation functions and to search for local twofold-rotation axes (Fig. 3). We detected such a dyad in the monoclinic crystal form 1; it corresponds either to peak *a*1 or to peak *a*1′ in Fig. 3(*a*) and is perpendicular to the twofold axis of the monoclinic crystal symmetry. This particular arrangement of a crystallographic and a proper noncrystallographic axis results in a pseudo-rotation axis which is perpendicular to both [peak *a*1′ in Fig. 3(*a*) in the case that the arbitrary assignment of peak *a*1 to the proper noncrystallographic axis was correct].

In the trigonal crystal form (Fig. 3*d*), we observed a similar 222 system consisting of a proper noncrystallographic twofold axis (peak *d*1), a crystallographic twofold axis and a pseudo-rotation axis (peak *d*1′). In this case, however, the whole arrangement occurs three times owing to the presence of threefold symmetry in the *c* direction (Fig. 3*d*).

Taken together, the self-rotation functions of crystal forms 1 and 4 can be completely explained on the basis of the presence of one *cg*Hle dimer per asymmetric unit, although in the case of the trigonal crystal form 4 this conclusion led to a $V_{\rm M}$ value and a solvent content that

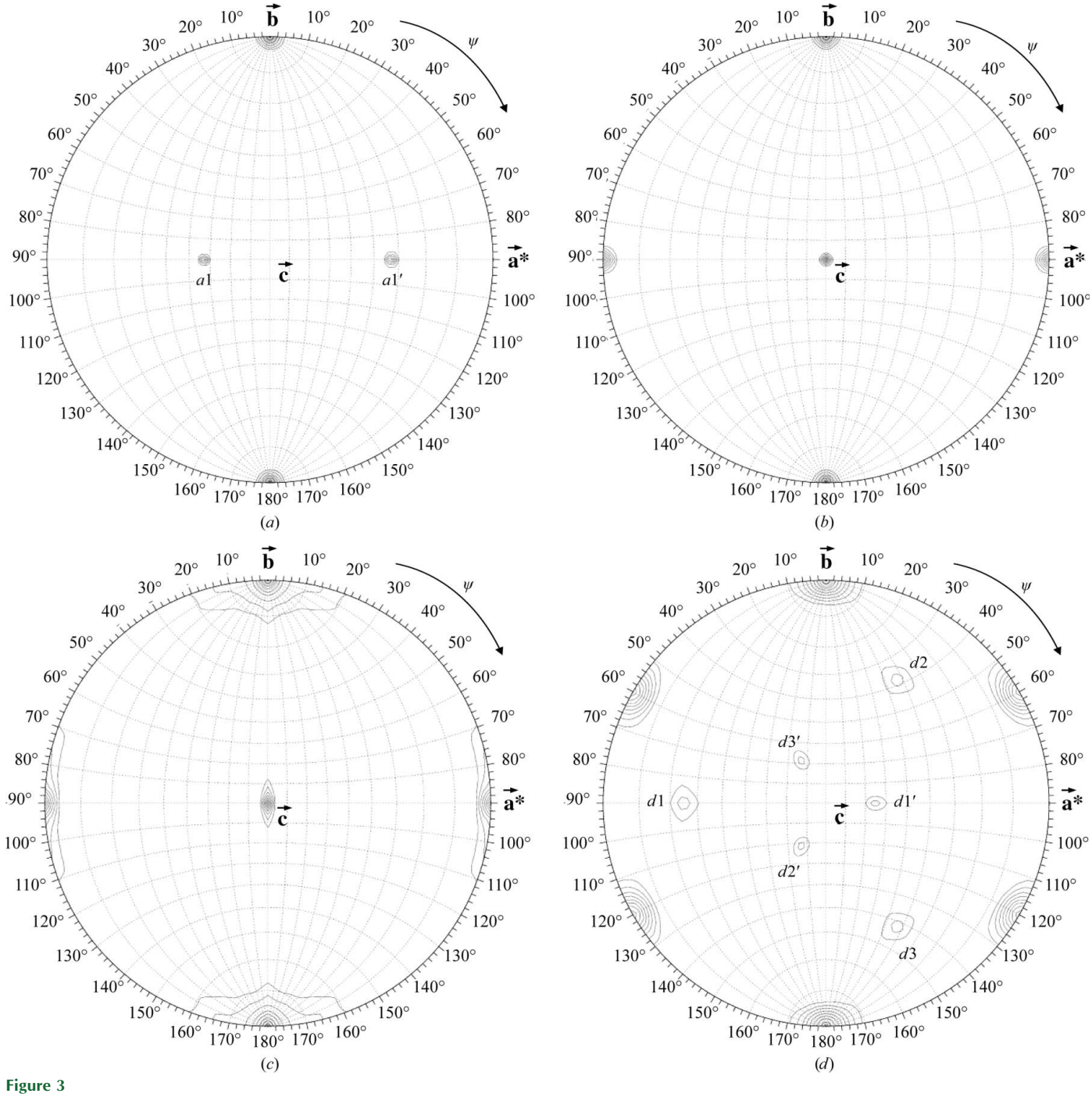

Figure 3
Search for 180° rotation axes in the four *cg*Hle crystal forms listed in Table 1. (*a*) Crystal form 1, (*b*) crystal form 2, (*c*) crystal form 3, (*d*) crystal form 4.

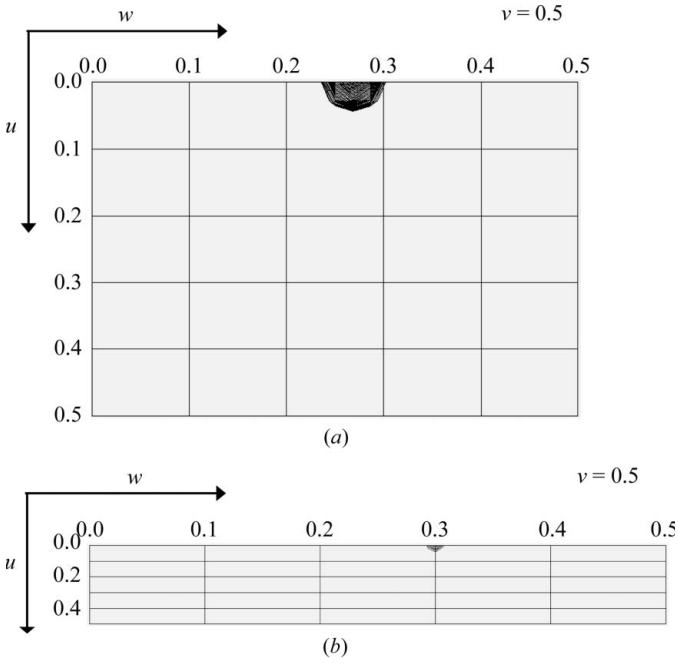

Figure 4
Native Patterson functions of the two orthorhombic *cg*Hle crystal forms: (*a*) crystal form 2 and (*b*) crystal form 3. The Harker sections at $v = 0.5$ are drawn. In both cases the Patterson peak visible on the Harker section is the second highest of the whole Patterson function after the origin peak.

were rather high (7.52 Å^3 Da^{-1} and 83.7%; Table 1). Since we did not determine crystal densities experimentally, this is a preliminary result that needs to be confirmed by the complete structure solution; however, the low protein content of this crystal form is consistent with the fact that its diffraction power (the high-resolution limit is 3.3 Å) was much poorer than those of the three other crystal forms (Table 1). Moreover, a search of the Protein Data Bank (Berman *et al.*, 2000) showed that the solvent content of 83.7% we determined for crystal form 4 is plausible as we detected more than 40 entries with solvent contents higher than 83%.

In the orthorhombic crystal form 2, no noncrystallographic twofold rotation axis could be found (Fig. 3*b*). This could mean that the local dyad relating the protomers of a *cg*Hle dimer is parallel to one of the three crystallographic 2_1 axes. In this case, the unit cell should contain pairs of *cg*Hle dimers with identical orientations related by pure translation vectors. To check this possibility, we calculated a native Patterson function in the resolution range 50–6 Å in which we detected a pseudo-origin peak with fractional coordinates 0, 0.5, 0.27, *i.e.* located on the Harker section $v = 0.5$ (Fig. 4*a*). This Patterson peak has a height of 24.1σ above the mean, which is about 50% of the height of the origin peak (46.2σ above the mean). Thus, the local twofold axis of the *cg*Hle dimer must be parallel to the crystallographic 2_1 axis in the *b* direction.

In the second orthorhombic crystal form (crystal form 3 in Table 1), again no noncrystallographic twofold rotation axis was obvious in the self-rotation map (Fig. 3*c*). However, in this case an analysis of the native Patterson functions was less clear: we calculated such maps in various resolution ranges, but two weak pseudo-origin peaks were only visible under low-resolution conditions. One of these peaks has a height of 8.1σ above the mean, compared with 66.9σ above the mean for the origin peak, and lies on the $v = 0.5$ Harker section (Fig. 4*b*). It is probable that the point-symmetry axes of the two corresponding *cg*Hle dimers are only approximately parallel to the crystallographic *b* axis. A further Patterson peak with a height of 3.28σ above the mean, significantly higher than the noise peaks, appeared at 0.28, 0, 0, *i.e.* not on a Harker section. It may be that this peak relates two *cg*Hle dimers of similar orientation within the asymmetric unit. Taken together, this would mean that the asymmetric unit of crystal form 3 contains four *cg*Hle protomers. The corresponding packing density is relatively high (40.1% solvent content), which correlates with the relatively good diffraction power of these crystals (Table 1).

In summary, the outlined crystal-packing analyses are plausible; whether they are really correct will be become apparent from the corresponding crystal structures, which we are currently determining.

We are grateful to the staff of the EMBL Outstation in Hamburg and of BESSY in Berlin for support during X-ray diffraction experiments and to Sabine Lohmar for excellent technical assistance.

References

Berman, H. M., Westbrook, J., Feng, Z., Gilliland, G., Bhat, T. N., Weissig, H., Shindyalov, I. N. & Bourne, P. E. (2000). *Nucleic Acids Res.* **28**, 235–242.
Bradford, M. M. (1976). *Anal. Biochem.* **72**, 248–254.
Collaborative Computational Project, Number 4 (1994). *Acta Cryst.* D**50**, 760–763.
Harp, J. M., Hanson, B. L., Timm, D. E. & Bunick, G. J. (1999). *Acta Cryst.* D**55**, 1329–1334.
Hermann, T. (2003). *J. Biotechnol.* **104**, 155–172.
Ikeda, M. & Nakagawa, S. (2003). *Appl. Microbiol. Biotechnol.* **62**, 99–109.
Kalinowski, J. *et al.* (2003). *J. Biotechnol.* **104**, 5–25.
Kanehisa, M., Araki, M., Goto, S., Hattori, M., Hirakawa, M., Itoh, M., Katayama, T., Kawashima, S., Okuda, S., Tokimatsu, T. & Yamanishi, Y. (2008). *Nucleic Acids Res.* **36**, D480–D484.
Marchler-Bauer, A. *et al.* (2007). *Nucleic Acids Res.* **35**, D237–D240.
Matthews, B. W. (1968). *J. Mol. Biol.* **33**, 491–497.
Mirza, I. A., Nazi, I., Korczynska, M., Wright, G. D. & Berghuis, A. M. (2005). *Biochemistry*, **44**, 15768–15773.
Ollis, D. L., Cheah, E., Cygler, M., Dijkstra, B., Frolow, F., Franken, S. M., Harel, M., Remington, S. J., Silman, I., Schrag, J., Sussman, J. L., Verschueren, K. H. G. & Goldman, A. (1992). *Protein Eng.* **5**, 197–211.
Onaca, C., Kieninger, M., Engesser, K.-H. & Altenbuchner, J. (2007). *J. Bacteriol.* **189**, 3759–3767.
Ostwald, W. (1897). *Z. Phys. Chem.* **22**, 289–330.
Otwinowski, Z. & Minor, W. (1997). *Methods Enzymol.* **276**, 307–326.
Park, S. D., Lee, J. Y., Kim, Y., Kim, J. H. & Lee, H. S. (1998). *Mol. Cells*, **8**, 286–294.
Rückert, C., Pühler, A. & Kalinowski, J. (2003). *J. Biotechnol.* **104**, 213–228.
The UniProt Consortium (2008). *Nucleic Acids Res.* **36**, D190–D195.
Tong, L. & Rossmann, M. G. (1997). *Methods Enzymol.* **276**, 594–611.
Volff, J. N., Eichenseer, C., Viell, P., Piendl, W. & Altenbuchner, J. (1996). *Mol. Microbiol.* **21**, 1037–1047.
Wang, M., Liu, L., Wang, Y., Wei, Z., Zhang, P., Li, Y., Jiang, X., Xu, H. & Gong, W. (2007). *Biochem. Biophys. Res. Commun.* **363**, 1050–1056.